

Efficient iterative solution of the discrete dipole approximation for magnetodielectric scatterers

Patrick C. Chaumet^{1,*} and Adel Rahmani²

¹*Institut Fresnel (UMR 6133), Université Paul Cézanne, Avenue Escadrille Normandie-Niemen, F-13397 Marseille, France*

²*Department of Mathematical Sciences and the Institute for Nanoscale Technology, University of Technology, Sydney, Broadway NSW 2007, Australia*

*Corresponding author: patrick.chaumet@fresnel.fr

Received December 16, 2008; accepted January 30, 2009;
 posted February 19, 2009 (Doc. ID 105433); published March 18, 2009

The discrete dipole approximation (DDA) has been widely used to study light scattering by nonmagnetic objects. The electric field inside an arbitrary scatterer is found by solving a dense, symmetric, linear system using, in general, an iterative approach. However, when the scatterer has a nonzero magnetic susceptibility, the linear system becomes nonsymmetric, and some of the most commonly used iterative methods fail to work. We study the scattering of light by objects with both electric and magnetic linear responses and discuss the efficiency of several iterative solvers for the nonsymmetric DDA. © 2009 Optical Society of America
 OCIS codes: 260.2110, 290.0290.

The scattering of an electromagnetic (EM) wave by an arbitrary object can be described using the discrete dipole approximation (DDA, also called the coupled dipole method) [1]. In the traditional form of the DDA, a nonmagnetic scatterer is discretized into a collection of electric dipoles over a cubic lattice [2–4]. At the heart of the DDA lies the resolution of a dense, symmetric, linear system of size $3N \times 3N$, where N is the number of electric dipoles. Often the system is too large to be solved by direct inversion, and iterative methods are used. A comparison of the efficiency of iterative methods in the DDA for nonmagnetic scatterers was done by Flatau [5], using the parallel iterative methods (PIM) package [6]. Note that there were errors in the implementation of some of the methods within PIM (missing complex conjugates in inner products), most notably the quasi-minimal residual (QMR) method. Indeed, while Flatau reported that QMR often failed to converge, in our experience, QMR is one of the most robust and efficient iterative methods for the DDA. Recent studies by Fan *et al.* also confirm the efficiency of QMR [7].

The DDA can also be used with magnetic materials, provided it is modified to include magnetic dipoles [8,9]. Consider a scatterer discretized into N polarizable subunits. For a given incident electromagnetic field $\{\mathbf{E}_{\text{inc}}, \mathbf{H}_{\text{inc}}\}$, the local fields at the i th subunit, located at \mathbf{r}_i , are given as

$$\mathbf{E}(\mathbf{r}_i) = \mathbf{E}_{\text{inc}}(\mathbf{r}_i) + \sum_{j \neq i} [\mathbf{G}^{\text{ee}}(\mathbf{r}_i, \mathbf{r}_j) \alpha^e(\mathbf{r}_j) \mathbf{E}(\mathbf{r}_j) + \mathbf{G}^{\text{em}}(\mathbf{r}_i, \mathbf{r}_j) \alpha^m(\mathbf{r}_j) \mathbf{H}(\mathbf{r}_j)] \quad (1)$$

$$\mathbf{H}(\mathbf{r}_i) = \mathbf{H}_{\text{inc}}(\mathbf{r}_i) + \sum_{j \neq i} [\mathbf{G}^{\text{me}}(\mathbf{r}_i, \mathbf{r}_j) \alpha^e(\mathbf{r}_j) \mathbf{E}(\mathbf{r}_j) + \mathbf{G}^{\text{mm}}(\mathbf{r}_i, \mathbf{r}_j) \alpha^m(\mathbf{r}_j) \mathbf{H}(\mathbf{r}_j)], \quad (2)$$

where the \mathbf{G} quantities are field susceptibility tensors (FSTs) [10] and α^e and α^m are the electric and

magnetic polarizabilities of subunit i [8], which for the sake of simplicity we will take as scalars. Notice that in cgs the FSTs satisfy $\mathbf{G}^{\text{ee}} = \mathbf{G}^{\text{mm}}$ and $\mathbf{G}^{\text{em}} = -\mathbf{G}^{\text{me}}$. The size of the linear system is now $6N \times 6N$, and because of the cross terms (electric field created by the induced magnetic polarization and vice versa) the system is no longer symmetric. As a consequence, some of the standard iterative methods, such as the conjugate gradient method, are no longer suitable.

Formally, deriving the local fields amounts to solving the linear system

$$\mathbf{A}\mathbf{x} = \mathbf{b}, \quad (3)$$

where vectors \mathbf{x} and \mathbf{b} have length $6N$ and contain the induced EM local fields and the incident EM fields, respectively. The nonsymmetric matrix \mathbf{A} is constructed from the FSTs [8] and can be written as

$$\mathbf{A} = \begin{pmatrix} \mathbf{I} & \mathbf{0} \\ \mathbf{0} & \mathbf{I} \end{pmatrix} - \begin{pmatrix} \mathbf{M} & \mathbf{K} \\ -\mathbf{K} & \mathbf{M} \end{pmatrix} \begin{pmatrix} \alpha^e & \mathbf{0} \\ \mathbf{0} & \alpha^m \end{pmatrix}, \quad (4)$$

where \mathbf{M} is a $3N \times 3N$ symmetric matrix block containing the linear response of the electric (magnetic) field to the electric (magnetic) polarization induced inside the scatterer, and \mathbf{K} , a $3N \times 3N$ antisymmetric matrix block, describes the cross responses (electric field response to a magnetic polarization and vice versa). α^e and α^m contain the electric and magnetic polarizabilities associated with the polarizable subunits forming the scatterer [8]. If the scatterer is made of isotropic materials, matrices α^e and α^m are diagonal. Note that unlike the nonmagnetic case, it is not generally possible to solve for the dipole moments rather than the fields, because this would mean having the inverse of the polarizabilities on the diagonal of the matrix, which is sound only if all the polarizabilities are nonzero. This means that the permittivity and the permeability must be different from 1 (or their corresponding values for the background medium) for every single subunit forming the scatterer.

We now proceed to solve Eq. (3) using two categories of algorithms. We first consider four of the more standard iterative methods [11]: the stabilized version of the biconjugate gradient (BICGSTAB), the QMR, the transpose-free quasi-minimal residual (TFQMR), and the restarted version of the generalized minimal residual method (GMRES) with 50 basis functions. We implemented these methods from the corresponding algorithms given in the PIM paper [6]. We also consider “hybrid” methods that combine the properties of two or more traditional methods. Two algorithms labeled QMRCGSTAB1 and QMRCGSTAB2 are QMR variants of the BICGSTAB algorithm [12]. The two final methods we consider are labeled GPBICG and GPBICG(m, l), which are refinements of the biconjugate gradient method [13]. For a given approximate solution \mathbf{x}_* to Eq. (3), we define the residual as

$$r = \|\mathbf{Ax}_* - \mathbf{b}\|/\|\mathbf{b}\|. \quad (5)$$

For each method the iterative process is terminated once $r < \epsilon$, where ϵ is a prescribed tolerance. All the iterative algorithms require two main types of computations: vector inner products and matrix-vector products (MVPs). Since for a large number of dipoles the most time-consuming operation is the MVP, our metric will be the number of MVPs required by each method to achieve $r < \epsilon$. Notice that depending on the iterative method, one or two MVPs are computed per iteration.

To illustrate the performance of the various iterative solvers we consider the scattering of an electro-

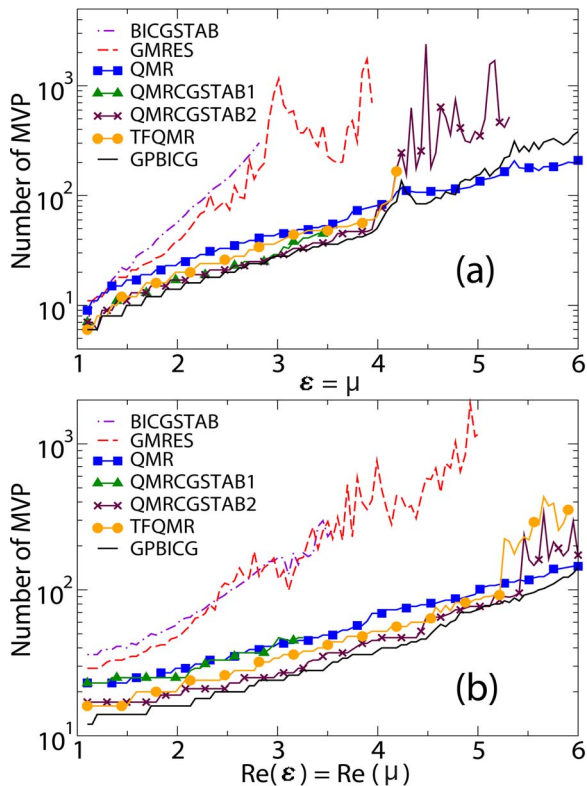


Fig. 1. (Color online) Number of MVPs versus $\epsilon = \mu$ for a homogenous sphere (see text for detail). (a) The sphere has no absorption: $\text{Im}(\epsilon) = \text{Im}(\mu) = 0$. (b) $\text{Im}(\epsilon) = \text{Im}(\mu) = 1$.

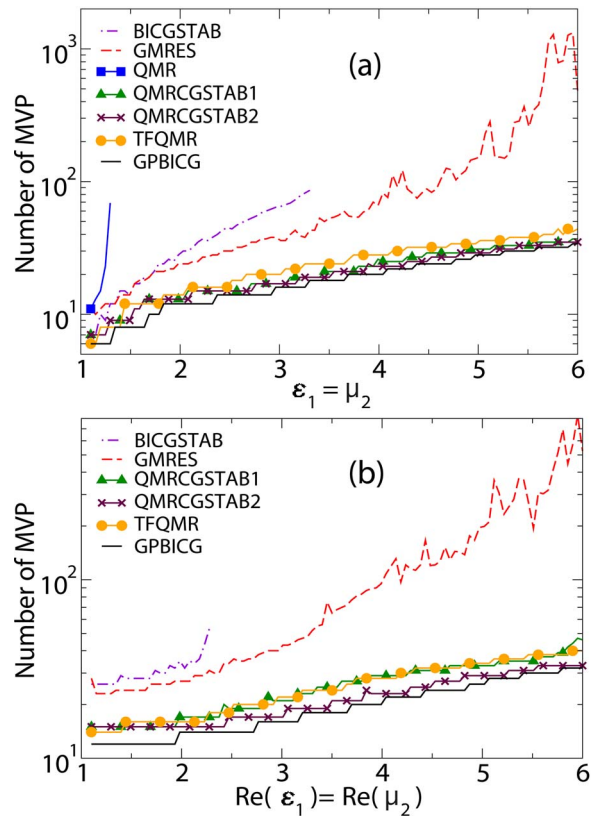


Fig. 2. (Color online) Number of MVPs versus $\epsilon_1 = \mu_2$ ($\epsilon_2 = \mu_1 = 1$) for an inhomogeneous sphere (see text for detail). (a) The sphere has no absorption. (b) $\text{Im}(\epsilon_1) = \text{Im}(\mu_2) = 1$.

magnetic plane wave (wavelength λ) by a spherical particle, and we compute the number of MVPs required to achieve a prescribed tolerance ϵ . A lack of data points for a given method indicates failure to converge. The first scatterer is a sphere of radius $a = \lambda/4$, discretized in $N = 4224$ subunits, and we study the number of MVPs needed to solve the linear system Eq. (4) versus the permittivity and permeability of the sphere (Fig. 1). The prescribed tolerance is fixed to $\epsilon = 10^{-5}$. Note that the computation is also stopped if convergence has not been reached after 5000 MVPs. Figure 1(a) pertains to a lossless material, whereas Fig. 1(b) corresponds to a lossy scatterer with $\text{Im}(\epsilon) = \text{Im}(\mu) = 1$. In Fig. 1(a) we can see that as ϵ and μ increase, the first methods to fail to achieve convergence are BICGSTAB, QMRCGSTAB1, and GMRES. The most robust methods are QMR and GPBICG, for which convergence is achieved even for the larger values of the permittivity and permeability considered here. Notice that for low values of ϵ and μ GPBICG requires less iteration than QMR to converge, whereas for large values of ϵ and μ the opposite is true. When we introduce material losses [Fig. 1(b)] convergence is improved for all the methods. This is a common feature of the DDA, as losses help dampen the morphological resonances of the scatterer, leading to a faster convergence. Nevertheless QMR and GPBICG are still the most efficient methods overall for large values of (ϵ, μ) .

In Fig. 2 we consider an inhomogeneous sphere of radius $a = \lambda/2$, discretized in $N = 4224$ subunits. The

upper half of the sphere (material 1) is a dielectric ($\mu_1=1$), and the lower half of the sphere (material 2) is magnetic ($\varepsilon_2=1$). This interesting case allows us to illustrate the behavior of the methods when two objects with different natures (dielectric or magnetic) are strongly coupled. The matrix containing the polarizabilities of the subunits now has many zeroes on its diagonal. Unlike in the previous example, in this case QMR performs very poorly, failing to converge even for a moderate value of the optical constants [Fig. 2(a)], and does not converge at all in the presence of absorption [Fig. 2(b)]. BICGSTAB and GMRES also perform poorly. On the other hand, the four remaining methods (QMRCGSTAB1, QMRCGSTAB2, TFQMR, and GPBICG) behave in a similar way, with GPBICG slightly better when absorption is present [Fig. 2(b)].

We now consider a larger sphere of radius $a=2\lambda$ and discretized in $N=268096$ subunits with a prescribed tolerance fixed to $\epsilon=10^{-3}$. Notice that this sphere has a large-size parameter (around 12). The case of dielectric spheres with large-size parameters has recently been studied, in the nonmagnetic case, by Yurkin *et al.* [14]. These authors showed that QMR was more robust than BICG and BICGSTAB and that an increase in the permittivity dramatically

decreases the performance of the iterative method. Figure 3(a) shows that in the magnetic case only five of the methods can potentially be used, although BICGSTAB still performs poorly, and so does QMRCGSTAB2. For this configuration the only method that always converges is GPBICG. In Fig. 3(b) we consider a sphere with the same geometric parameters as in the previous example but with one half of the sphere made of nonmagnetic material and the other half made of magnetic material (with the same material constants as in Fig. 2). For this large, inhomogeneous sphere, we find that only three of the methods are able to deal with even very weak values of (ε, μ) , and only GPBICG achieves convergence for larger values of the permittivity and the permeability.

Finally we note that there exists a hybrid method based on BICGSTAB and GPBICG [13] called GPBICG(m, l). Roughly, the method consists in using BICGSTAB for m steps and subsequently using GPBICG for l iteration steps. Combination of m and l should be chosen according to the nature of the problem. In our case we have tried all combinations for $m \leq 3$ and $l \leq 3$. We have not plotted the corresponding results, as it appears that the standard GPBICG is always the most efficient iterative algorithm for the cases we tested.

In conclusion, we have shown that GPBICG is the most versatile and robust iterative method to solve the nonsymmetric linear system associated with the formulation of the DDA for magnetodielectric scatterers.

References

1. E. M. Purcell and C. R. Pennypacker, *Astrophys. J.* **186**, 705 (1973).
2. B. T. Draine, *Astrophys. J.* **333**, 848 (1988).
3. B. T. Draine and P. J. Flatau, *J. Opt. Soc. Am. A* **11**, 1491 (1994).
4. P. C. Chaumet, A. Sentenac, and A. Rahmani, *Phys. Rev. E* **70**, 036606-6 (2004).
5. P. J. Flatau, *Opt. Lett.* **22**, 1205 (1997).
6. R. D. Da Cunha and T. Hopkins, *Appl. Numer. Math.* **19**, 33 (1995).
7. Z. H. Fan, D. X. Wang, R. S. Chan, and E. K. N. Yung, *Microwave Opt. Technol. Lett.* **48**, 1741 (2006).
8. P. C. Chaumet and A. Rahmani, *J. Quant. Spectrosc. Radiat. Transf.* **110**, 22 (2009).
9. P. C. Chaumet and A. Rahmani, *Opt. Express* **17**, 2224 (2009).
10. G. S. Agarwal, *Phys. Rev. A* **11**, 230 (1975).
11. Y. Saad, *Iterative Methods for Sparse Linear Systems* (SIAM, 2003).
12. T. F. Chan, E. Gallopoulos, V. Simoncini, T. Szeto, and C. H. Tong, *SIAM J. Sci. Comput. (USA)* **15**, 338 (1994).
13. J. Tang, Y. Shen, Y. Zheng, and D. Qiu, *Coastal Eng.* **51**, 143 (2004).
14. M. A. Yurkin, V. P. Maltsev, and A. G. Hoekstra, *J. Quant. Spectrosc. Radiat. Transf.* **106**, 546 (2007).

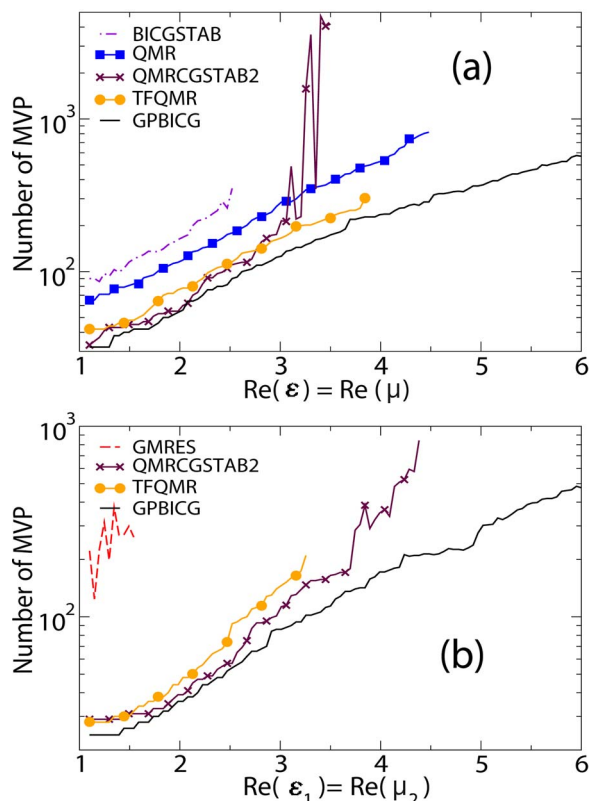


Fig. 3. (Color online) Sphere of radius $a=2\lambda$. (a) $\text{Im}(\varepsilon)=\text{Im}(\mu)=1$. (b) $\text{Im}(\varepsilon_1)=\text{Im}(\mu_2)=1$